Combination therapy with oral antiviral and anti-inflammatory drugs improves the efficacy of delayed treatment in a COVID-19 hamster model

Michihito Sasaki,[a,b,*] Tatsuki Sugi,[c,d] Shun Iida,[e] Yuichiro Hirata,[e] Shinji Kusakabe,[f,g] Kei Konishi,[f,g] Yukari Itakura,[a,b] Koshiro Tabata,[a,b] Mai Kishimoto,[a,l] Hiroko Kobayashi,[a] Takuma Ariizumi,[a] Kittiya Intaruck,[a] Haruaki Nobori,[g] Shinsuke Toba,[f,g] Akihiko Sato,[b,f,g] Keita Matsuno,[d,h,i] Junya Yamagishi,[c,d,i] Tadaki Suzuki,[e] William W. Hall,[b,d,j,k] Yasuko Orba,[a,b,d,f,i] and Hirofumi Sawa[b,d,f,i,k]

[a]Division of Molecular Pathobiology, International Institute for Zoonosis Control, Hokkaido University, Sapporo, Japan
[b]Institute for Vaccine Research and Development (HU-IVReD), Hokkaido University, Sapporo, Japan
[c]Division of Collaboration and Education, International Institute for Zoonosis Control, Hokkaido University, Sapporo, Japan
[d]International Collaboration Unit, International Institute for Zoonosis Control, Hokkaido University, Sapporo, Japan
[e]Department of Pathology, National Institute of Infectious Diseases, Tokyo, Japan
[f]Division of Anti-Virus Drug Research, International Institute for Zoonosis Control, Hokkaido University, Sapporo, Japan
[g]Drug Discovery & Disease Research Laboratory, Shionogi & Co., Ltd., Osaka, Japan
[h]Division of Risk Analysis and Management, International Institute for Zoonosis Control, Hokkaido University, Sapporo, Japan
[i]One Health Research Center, Hokkaido University, Sapporo, Japan
[j]National Virus Reference Laboratory, School of Medicine, University College of Dublin, Ireland
[k]Global Virus Network, Baltimore, Maryland, USA

eBioMedicine
2024;99: 104950
Published Online 30 December 2023
https://doi.org/10.1016/j.ebiom.2023.104950

Summary

Background Pulmonary infection with SARS-CoV-2 stimulates host immune responses and can also result in the progression of dysregulated and critical inflammation. Throughout the pandemic, the management and treatment of COVID-19 has been continuously updated with a range of antiviral drugs and immunomodulators. Monotherapy with oral antivirals has proven to be effective in the treatment of COVID-19. However, treatment should be initiated in the early stages of infection to ensure beneficial therapeutic outcomes, and there is still room for further consideration on therapeutic strategies using antivirals.

Methods We studied the therapeutic effects of monotherapy with the oral antiviral ensitrelvir or the anti-inflammatory corticosteroid methylprednisolone and combination therapy with ensitrelvir and methylprednisolone in a delayed dosing model of hamsters infected with SARS-CoV-2.

Findings Combination therapy with ensitrelvir and methylprednisolone improved respiratory conditions and reduced the development of pneumonia in hamsters even when the treatment was started after 2 days post-infection. The combination therapy led to a differential histological and transcriptomic pattern in comparison to either of the monotherapies, with reduced lung damage and down-regulation of expression of genes involved in the inflammatory response. Furthermore, we found that the combination treatment is effective in case of infection with either the highly pathogenic delta or circulating omicron variants.

Interpretation Our results demonstrate the advantage of combination therapy with antiviral and corticosteroid drugs in COVID-19 treatment from the perspective of lung pathology and host inflammatory responses.

Funding Funding bodies are described in the Acknowledgments section.

Keywords: SARS-CoV-2; COVID-19; Antiviral therapy; Corticosteroid; Hamster; Delayed treatment

*Corresponding author. Division of Molecular Pathobiology, International Institute for Zoonosis Control, Hokkaido University, Sapporo, Japan.
E-mail address: m-sasaki@czc.hokudai.ac.jp (M. Sasaki).
[l]Current affiliation: Laboratory of Veterinary Microbiology, Graduate School of Veterinary Science, Osaka Metropolitan University, Osaka, Japan.

Research in context

Evidence before this study

We searched PubMed for studies published in English from database inception to February 15th, 2022, using the search terms ("SARS-CoV-2" AND "Antivirals" AND "Anti-Inflammatory Agents" AND "Animals"). Our search identified multiple studies about combination therapies with antivirals, antibodies and anti-inflammatory agents. However, there is a lack of information about the therapeutic effect of oral combination treatment with antiviral and anti-inflammatory agents in animal models of COVID-19.

Added value of this study

We showed that delayed antiviral monotherapy resulted in reduced therapeutic efficacy in SARS-CoV-2 infected hamsters. However, we found that combination therapy with antiviral and anti-inflammatory corticosteroid drugs controlled a wide range of host inflammatory responses, improved the lung pathology, and ameliorated clinical aspects of COVID-19 compared to the effects of ETV or mPSL monotherapies in the delayed dosing model.

Implications of all the available evidence

Our study has implications for clinical practice. Combination therapy with antiviral and anti-inflammatory corticosteroid drugs restricted both viral spread and hyperinflammation leading to better outcomes in COVID-19. Since both drugs are available as oral medications, this combination therapy could provide a clinical and potent therapeutic option for the treatment of COVID-19.

Introduction

Coronavirus disease 2019 (COVID-19), caused by infection with severe acute respiratory syndrome coronavirus 2 (SARS-CoV-2), is linked to mild-to-severe respiratory distress, pneumonia, and death. Bronchial and alveolar epithelial cells are the major target cells for SARS-CoV-2 infection, and these cells trigger host innate immune and inflammatory responses in the lungs.[1] Following viral replication, interferons and cytokines are produced and released from infected and bystander epithelial cells and immune cells, leading to the activation and pulmonary infiltration of immune cells including macrophages and neutrophils.[2] Although a proper immune response orchestrates the antiviral state and attenuates tissue damage by viral infection, severe COVID-19 shows an imbalanced and hyperactive host immune response characterised by defects in the type I interferon response and the dysregulated release of pro-inflammatory cytokines, resulting in deleterious inflammation.[3,4] Overall, the inflammatory response to SARS-CoV-2 infection plays a pivotal role in the pathogenesis of severe COVID-19.

Several medications have been employed for COVID-19 therapy.[5] In the early phase of infection, oral antiviral agents such as nirmatrelvir and molnupiravir are recommended for treating non-hospitalized patients to reduce the viral load and the risk of COVID-19-related hospitalization.[6,7] In addition, ensitrelvir (ETV) reduces the time to resolution of COVID-19 symptoms, and it is currently approved as an oral antiviral medication for COVID-19 in Japan.[8] For therapeutic efficacy, it is advisable that these oral antiviral medications are initiated as soon as possible after the onset of symptoms.[5] In the later stages of infection, immunomodulators are expected to circumvent tissue damage induced by the inflammatory response observed exclusively in severe COVID-19. In such a situation, dexamethasone, an anti-inflammatory corticosteroid, was shown to reduce the mortality rate in hospitalised patients with COVID-19 requiring supplemental oxygen.[9] Methylprednisolone (mPSL) is also used as an alternative corticosteroid for the same purpose; however, evidence of the efficacy of mPSL in severe COVID-19 remains insufficient because of the small sample sizes in clinical trials.[10] Because corticosteroids cause immunosuppression and increase viral loads, this treatment can be harmful rather than beneficial in patients with mild-to-moderate COVID-19.[11,12] Meanwhile, combination therapy with the intravenous antiviral drug remdesivir (RDV) and immunomodulators produced better outcomes than treatment with RDV or immunomodulator alone in severe diseases.[13,14] However, little is known about the therapeutic impact of combination therapy with oral antiviral agents and immunomodulators in either mild-to-moderate and severe COVID-19.

Syrian hamsters are highly susceptible to infection with SARS-CoV-2, and they are widely used in *in vivo* studies of COVID-19. To date, the hamster has proven to be the most reliable animal model for studying COVID-19 pathophysiology and therapeutics. In preclinical studies, oral antiviral agents reduced viral loads and improved lung pathology in recipient hamsters infected with SARS-CoV-2.[15–17] Recently, we demonstrated that post-exposure treatment with ETV in SARS-CoV-2-infected hamsters resulted in reduced viral replication and alleviated clinical signs.[18] Treatment with corticosteroids also improved pathology but increased viral loads and delayed clearance of virus in the lungs of hamsters.[19–21] Moreover, two studies examined the combinations of RDV plus mPSL[19] and neutralizing monoclonal antibody plus dexamethasone,[21] and observed favourable therapeutic effects compared to those of monotherapy.

Considering the relationship between virus replication and the host inflammatory response in lungs, it is desirable to initiate treatment with oral antiviral drugs

early after the onset of infection. However, treatment in clinical settings is sometimes initiated in the context of extensive SARS-CoV-2 replication in the respiratory tracts of patients. In this study, we investigated the influence of delaying oral antiviral ETV treatment on therapeutic efficacy using a SARS-CoV-2-infected hamster model. We then evaluated and characterised the therapeutic effect of oral combination treatment with ETV and mPSL in a delayed dosing model using histopathological and transcriptome analyses.

Methods

Cells

Vero-TMPRSS2 cells [Vero E6 cells (CRL-1586, ATCC, RRID:CVCL_0574) stably expressing human TMPRSS2] and Vero-hACE2-TMPRSS2 (Vero E6 cells stably expressing human ACE2 and human TMPRSS2) were established using lentiviral vectors as previously described[22,23] and maintained in Dulbecco's Modified Eagle's Medium (DMEM) containing 10% foetal bovine serum (FBS). The cells were regularly confirmed to be negative for mycoplasma contamination by MycoAlert Mycoplasma Detection Kit (Lonza Bioscience).

Viruses

SARS-CoV-2 delta (strain TY11-927, lineage AY.122, GISAID: EPI_ISL_2158617) and omicron (strain TY41-795, lineage XBB.1, GISAID: EPI_ISL_ 15669344) variants were obtained from the National Institute of Infectious Diseases, Japan.

Compounds

ETV (also known as code S-217622, fumaric acid co-crystal form) was provided from Shionogi & Co., Ltd.[24] mPSL was obtained from the Tokyo Chemical Industry. RDV was obtained from Combi-Blocks.

Animal experiments

Sample sizes of 3 or 4 animals/group were determined based on prior *in vivo* studies, and no power calculations were performed. Animals were divided into three groups based on their body weights (high-, middle- and low-body weight strata) and randomly assigned to each treatment groups with same ratio to ensure a homogenous distribution of treatments over these strata. Animals were housed in sterile isolators under 12 h light/12 h dark cycles with free access to food and water. No blinding procedures were applied. Five-week-old male or female Syrian hamsters (Japan SLC) were intranasally inoculated with 1×10^4 pfu of SARS-CoV-2 in 200 μl of PBS under anaesthesia with isoflurane inhalation. ETV was suspended at 20 mg/ml in 0.5% (w/v) methyl cellulose 400. mPSL was solubilised as 100 mg/ml solution in dimethyl sulfoxide and suspended at 1 mg/ml in 0.5% (w/v) methyl cellulose 400. RDV was solubilised as a 100 mg/ml solution in dimethyl sulfoxide and suspended at 3 mg/ml in 12% (w/v) sulfobutylether-β-cyclodextrin, pH 5.0. Hamsters were orally administered twice daily with ETV (200 mg/kg) and/or mPSL (10 mg/kg) suspension for 5 days from 0, 1 or 2 dpi under anaesthesia with isoflurane inhalation. The dose of ETV was determined based on drug exposure in rodents in which no adverse effects were observed in safety studies.[25] For treatment with RDV, hamsters were intraperitoneally injected with RDV solution (15 mg/kg) at 2 and 3 dpi. Vehicle control hamsters were administered with 0.5% (w/v) methyl cellulose 400. A subset of hamsters at 4 dpi or 6 dpi were sacrificed for lung collection. The lung tissues were used for virus titration, gene expression assays and histopathological examination. Another subset of hamsters were monitored for up to 10 dpi for body weight change and subjected to blood collection at 18 dpi. Body weights of animals were monitored daily. The humane endpoint was established as body weight loss exceeding 30% or moribund state due to severe infection.

Ethics

The animal experiments with virus infection were performed in accordance with the National University Corporation, Hokkaido University Regulations on Animal Experimentation. The protocol was reviewed and approved by the Institutional Animal Care and Use Committee of Hokkaido University (approval no. 20-0060).

Microneutralization assay for SARS-CoV-2

To determine the titres of neutralizing antibody in hamsters, serum samples were collected from hamsters at 18 dpi and heated at 56 °C for 30 min to inactivate complement. Serial two-fold dilutions of serum samples in DMEM containing 2% FBS were incubated with 100 pfu of SARS-CoV-2 delta variant at 37 °C for 1 h. The serum-virus mixtures of 50 μl were then added to Vero-TMPRSS2 cells in 96 well plates. After 4 dpi, viral cytopathic effects were examined under an inverted microscope. The neutralization titre was defined as the reciprocal of the highest serum dilution that completely inhibited the virus cytopathic effects in Vero-TMPRSS2 cells.

Virus titration and quantitative RT-PCR (qRT-PCR) assays

Lungs from hamsters at 4 or 6 dpi were homogenised in PBS with TissueRuptor (Qiagen). A part of the whole lung homogenate was subjected to virus titration by plaque assays on Vero-TMPRSS2 for the delta variant and Vero-hACE2-TMPRSS2 for the omicron variant. The cell monolayers were inoculated with serial dilutions of the lung homogenates for 1 h at 37 °C. The cells were then overlaid with DMEM containing 2% FBS and 0.5% Bacto Agar (Becton Dickinson). At 2 days (for the delta variant) or 3 days (for the omicron variant)

post-inoculation, cells were fixed with 3.7% buffered formaldehyde and stained with 1% crystal violet. For measurement of host gene expression and viral RNA levels, total RNA was extracted from the homogenate with a combination of TRIzol LS (Invitrogen) and Direct-zol RNA MiniPrep kit (Zymo Research). RNA samples were analysed by qRT-PCR with Thunderbird Probe One-step qRT-PCR Kit (Toyobo) and QuantStudio 7 Flex Real-time PCR system (Applied Biosystems; Thermo Fisher Scientific). Target RNA levels were normalised to hamster *Actb* and calculated by the relative standard curve method. The copy numbers of hamster *Actb* and SARS-CoV-2 nucleocapsid genes were also estimated by the standard curve method. Primers and probes for hamster *Irf7* and *Oas2* were obtained as a PrimeTime Predesigned qPCR assay (Integrated DNA Technologies). Other primers and probes for hamster *Actb*, *Il6*, *Il10*, *Ccl2*, *Cxcl10*, and SARS-CoV-2 nucleocapsid genes were as previously described.[26–28]

Differentially expressed genes

For mRNA-seq analysis, total RNA samples from lungs at 4 dpi were subjected to library preparation using NEBNext Ultra II Directional RNA Library prep kit for Illumina (New England Biolabs) and sequenced on an Illumina NovaSeq 6000 with 150 base pair-end reads at Azenta. Raw mRNA-seq data were deposited to DDBJ with accession IDs DRR477693-DRR477707. Obtained mRNA-seq reads were processed with the nf-core/RNAseq pipeline.[29] Preprocessed paired reads were aligned to reference genomes with STAR (v2.7.10).[30] Genome data for Syrian Golden hamster (Ensemble MesAur1.0) and SARS-CoV-2 (Ensemble ASM985889v3 Wuhan-Hu-1 isolate), respectively, were used.[31] Gene level transcript abundances were estimated by Salmon (v1.9.0)[32] and tximport (v1.22).[33] Reads mapped to SARS-CoV-2 genome were removed in further analysis. Differentially expressed gene analysis was performed using DESeq2 (v1.34).[34] Differentially expressed genes were ranked with a *P*-value and the direction of fold change as described elsewhere[35] and ranked gene lists were used for geneset enrichment analysis[36] using ClusterProfiler (v4.2.2).[37] To utilise human genesets, hamster gene IDs were converted to human gene IDs by g:Profiler suite.[38] Genes with one-to-one ortholog relation, human genesets retrieved from Reactome Pathway[39] and CellMarker,[40] and cell type markers with evidence code "Experimental" were used for the analysis. For heatmap analysis, a DESeq2 normalised gene expression table was log2 transformed and was scaled in gene-wise manner to establish relative gene expression values (z-score).

Pulmonary function tests

Pulmonary function was assessed using a whole-body plethysmography system (Data Sciences International) as previously described.[41] In brief, hamsters were placed individually in unrestrained plethysmography chambers. After 30 s for acclimatisation, respiratory parameters were acquired over a 3-min period by using FinePointe software (Data Sciences International).

Histopathological examination

Lung tissues at 4 and 6 dpi were fixed in 3.7% formaldehyde in PBS and embedded in paraffin. To detect viral RNA in the paraffin sections, *in situ* hybridization was carried out using an RNA scope 2.5 HD Red Detection kit (Advanced Cell Diagnostics) with an antisense probe targeting the nucleocapsid gene of SARS-CoV-2 (Advanced Cell Diagnostics) as previously described.[42] To detect viral antigen in the sections, IHC was carried out using a rabbit monoclonal antibody for SARS-CoV nucleocapsid protein (40143-R001, clone #001, Sino Biological, RRID:AB_2827974) which cross-reacts with SARS-CoV-2 nucleocapsid protein. Specific antigen-antibody reactions were visualised by means of 3,3′-diaminobenzidine tetrahydrochloride staining using the Dako Envision system (Dako Cytomation). Histopathological severity score of pneumonia was determined based on the percentage of alveolar inflammation in a given area of a pulmonary section collected from each animal in each group using the following scoring system: 0, no inflammation; 1, affected area (≤1%); 2, affected area (>1%, ≤10%); 3, affected area (>10%, ≤50%); 4, affected area (>50%); an additional point was added when pulmonary oedema and/or alveolar haemorrhage was observed.[43] The average score for all lobes was calculated for each animal.

Statistics

Statistical differences between treatments in the experiments including an uninfected control were determined by one-way analysis of variance (ANOVA) with Tukey's test (Figs. 1c–e, i–l, 2d and e, 5a and b, 6e–j, Supplementary Figure S4c–f). Statistical differences between vehicle treated and drug-treated animals were determined by one-way ANOVA with Dunnett's test (Figs. 1f and g, 2c, f–i, 6a and b, Supplementary Figures S2 and S4a and b). When the data did not meet the ANOVA criteria, statistical analyses were conducted by Kruskal–Wallis test with the Dunn's multiple comparisons test (Figs. 3c, e and f, 6d). All statistical tests were carried out using Prism version 9.5.1 (GraphPad software).

Role of funders

The funders had no role in the study design, data collection, analysis, or interpretation, or any aspect pertinent to this study.

Results

Delayed treatment attenuates the therapeutic effect of ETV in hamsters

To examine the influence of delaying antiviral administration on COVID-19 treatment, hamsters were

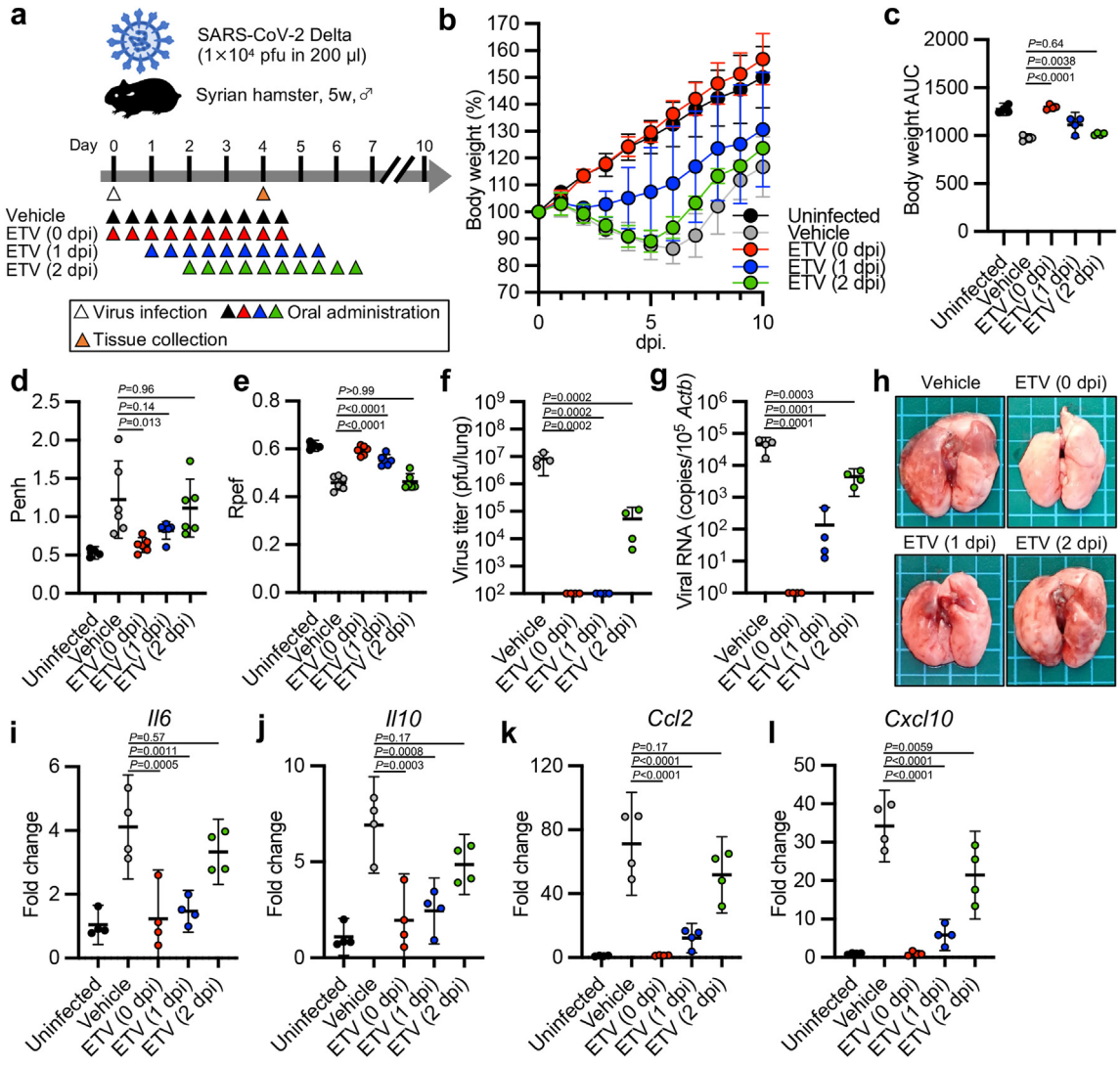

Fig. 1: **Differences in outcomes between immediate and delayed treatment with the antiviral drug ensitrelvir (ETV) in hamsters infected with SARS-CoV-2. a**, Schematic representation of the experimental design for antiviral treatment in the hamster model. Male hamsters were intranasally inoculated with 1×10^4 pfu of the SARS-CoV-2 delta variant. The hamsters were orally treated with ensitrelvir (ETV, 200 mg/kg) or vehicle alone b.i.d. for 5 days starting at the time of infection [ETV (0 dpi) and vehicle], 1 day post-infection (dpi) [ETV (1 dpi)], or 2 dpi [ETV (2 dpi)]. A group of hamsters was sacrificed at 4 dpi for tissue collection. Another subset of hamsters was monitored for 10 dpi for body weight changes. **b**, Body weight changes in uninfected and SARS-CoV-2-infected hamsters treated with ETV or vehicle (n = 4 for each group). **c**, Area under the curve (AUC) of body weight over time in (b) (n = 4 for each group). **d, e**, Enhanced pause (Penh) (d) and ratio of peak expiratory flow (Rpef) (e) in hamsters at 4 dpi were measured by whole-body plethysmography (n = 4 for the uninfected group, n = 6 for the other groups). **f**, Virus titres in the lungs of hamsters at 4 dpi were determined by the plaque assay (n = 4 for each group). **g**, Viral RNA copies in the lungs of hamsters at 4 dpi were quantified by quantitative RT-PCR (qRT-PCR) and normalised to those of *Actb* (n = 4 for each group). **h**, Gross observation of lungs at 4 dpi. Side length of squares, 5 mm. **i–l**, Relative gene expression of *Il6* (i), *Il10* (j), *Ccl2* (k), and *Cxcl10* (l) in infected hamster lungs at 4 dpi compared to that in the lungs of uninfected hamsters were examined using qRT-PCR (n = 4 for each group). Data were normalised to those of *Actb*. All graph shows mean and 95% confidence intervals (CIs) with each dot representing an individual animal. Statistics were calculated by one-way ANOVA with Tukey's test (c–e, i–l) and one-way ANOVA with Dunnett's test (f, g). *P* values versus vehicle-treated control are indicated in the graphs.

intranasally infected with SARS-CoV-2 and then orally treated for 5 days with ETV using three different starting times: immediately after inoculation to 4 days post-infection (dpi) [ETV (0 dpi)], from 1 to 5 dpi [ETV (1 dpi)], and from 2 to 6 dpi [ETV (2 dpi); Fig. 1a]. Hamsters treated with methyl cellulose 400 (vehicle)

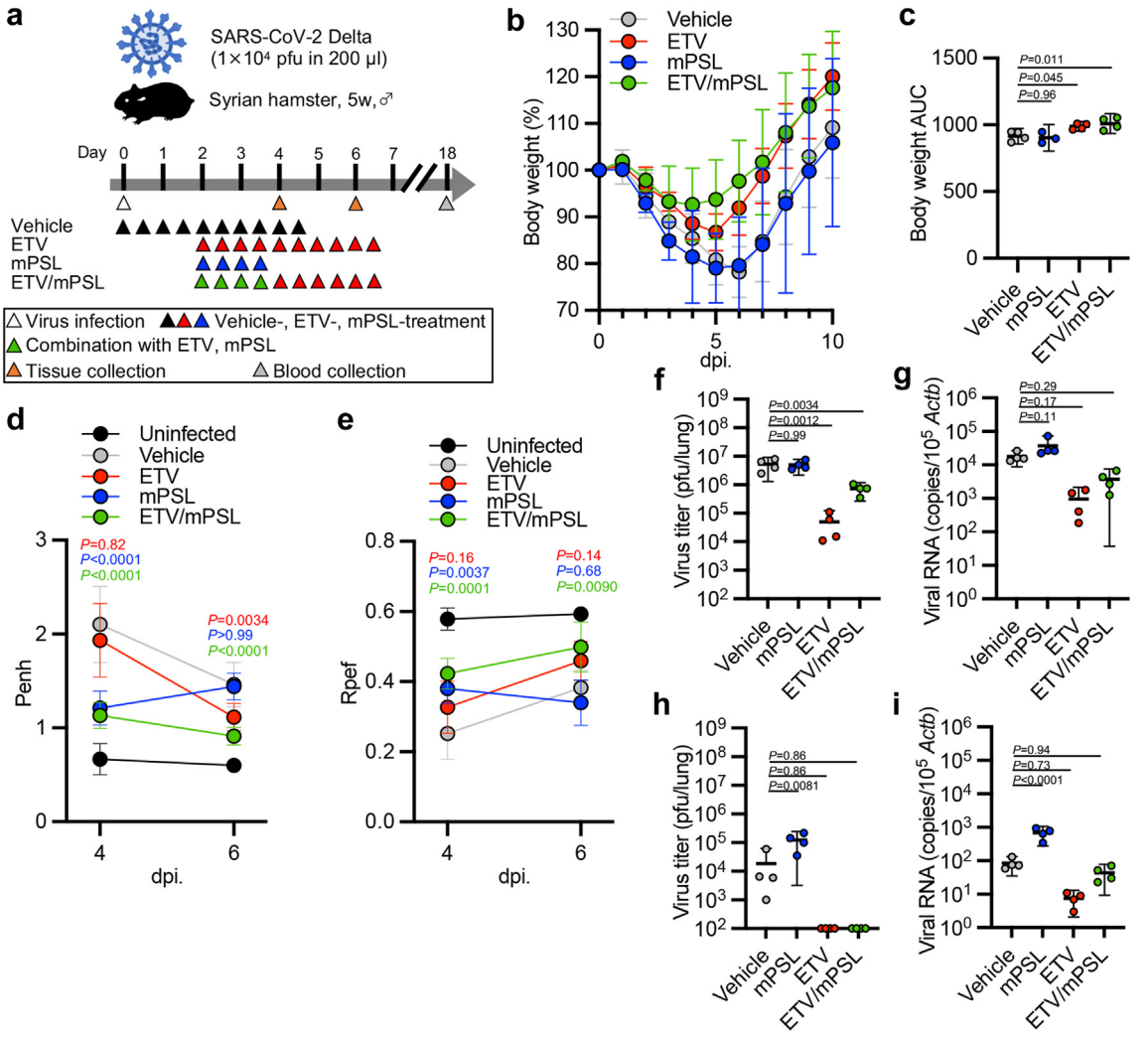

Fig. 2: **Therapeutic treatment of SARS-CoV-2 infection in hamsters with ETV and methylprednisolone (mPSL). a**, Schematic representation of the experimental design for treatment in the hamster model. Male hamsters inoculated with the SARS-CoV-2 delta variant were orally treated with ETV for 5 days (200 mg/kg, b.i.d., 2–6 dpi) and/or mPSL for 2 days (10 mg/kg, b.i.d., 2–3 dpi). A group of hamsters was sacrificed at 4 dpi for tissue collection. Another subset of hamsters was monitored for 10 dpi for body weight changes. **b**, Body weight changes in SARS-CoV-2-infected hamsters treated with ETV and/or mPSL (n = 4 for each group). **c**, AUC analysis of body weight over time in (b). One mouse in mPSL group reached humane endpoint at 7 dpi and was excluded from the analysis (n = 3 for mPSL, n = 4 for other groups). **d, e**, Enhanced pause (Penh) (d) and ratio of peak expiratory flow (Rpef) (e) in hamsters at 4 and 6 dpi were measured by whole-body plethysmography (n = 4 for the uninfected group, n = 6 for the other groups). **f–i**, Virus titres (f, h) and viral RNA copies (g, i) in the lungs of hamsters at 4 (f, g) and 6 dpi (h, i) (n = 4 for each group). Viral RNA copies were normalised to those of *Actb*. All graph shows mean and 95% CIs with each dot representing an individual animal. Statistics were calculated by one-way ANOVA with Dunnett's test (c–i). *P* values versus vehicle-treated control are indicated in the graphs.

were included as an untreated control group in this study. We used the SARS-CoV-2 delta variant (lineage AY.122), which is a highly pathogenic variant that causes severe pneumonia in hamsters.[42,44,45] Vehicle-treated hamsters exhibited body weight loss up to 6 dpi (Fig. 1b). Compared to vehicle-treated group, mice receiving ETV treatment from 0 dpi showed a slight reduction of body weight associated with the infection [mean AUC difference to ETV (0 dpi) of −323, 95% CI −420 to −226], whereas delayed treatment had limited ameliorating effects on body weight loss [mean AUC difference to ETV (2 dpi) of −43.8, 95% CI −141 to 53.3] (Fig. 1c). The respiratory condition of hamsters at 4 dpi was assessed by measuring the enhanced pause (Penh) and ratio of peak expiratory flow (Rpef) using whole-body plethysmography (Fig. 1d and e).

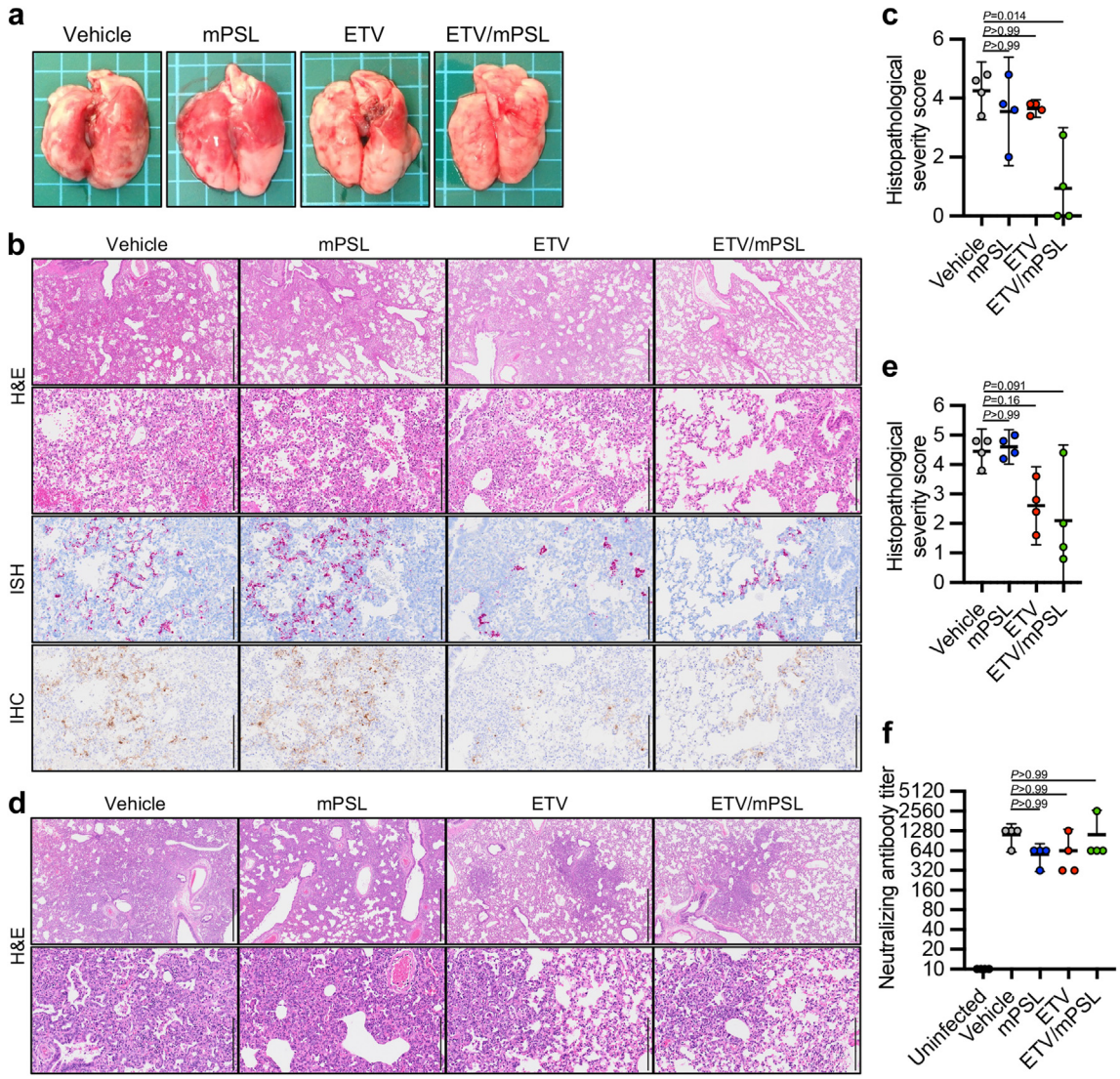

Fig. 3: **Histopathological findings in the lungs of SARS-CoV-2-infected hamsters receiving therapeutic treatment.** Male hamsters were infected with 1×10^4 pfu of the SARS-CoV-2 delta variant and treated b.i.d. with ETV (200 mg/kg) at 2–6 dpi and/or mPSL (10 mg/kg) at 2–3 dpi following the schedule shown in Fig. 2a. **a**, Gross observation of lungs from hamsters at 4 dpi. Side length of squares, 5 mm. **b**, Representative histopathological images of the lungs of hamsters at 4 dpi. Upper two panels, haematoxylin and eosin staining. The third from the top panels, *in situ* hybridization (ISH) targeting the nucleocapsid gene of SARS-CoV-2. Bottom panels, immunohistochemistry (IHC) targeting the nucleocapsid protein of SARS-CoV-2. Scale bars in the top panels, 1 mm. Scale bars in other panels, 200 μm. **c**, Histopathological severity score of pneumonia at 4 dpi based on the percent area of alveolitis in a given section (n = 4 for each group). **d**, Representative histopathological images of hamster lungs at 6 dpi. All panels display haematoxylin and eosin staining. Scale bars in the upper panels, 1 mm. Scale bars in lower panels, 200 μm. **e**, Histopathological severity score of pneumonia at 6 dpi based on the percent area of alveolitis in a given section (n = 4 for each group). **f**, Neutralizing antibody titres in hamster serum collected at 18 dpi (n = 4 for each group). All graph shows mean and 95% CIs with each dot representing an individual animal. Statistics were calculated by Kruskal–Wallis test with Dunn's test (c, e, f). *P* values versus vehicle-treated control are indicated in the graphs.

Compared to vehicle-treated group, ETV treatment inhibited the increase in Penh and decrease in Rpef associated with SARS-CoV-2 infection [mean Penh difference to ETV (0 dpi) of 0.592, 95% CI 0.998–1.08], indicating improvement in the respiratory conditions, but this effect was limited in the delayed-treatment groups [mean Penh difference to ETV (2 dpi) of 0.108, 95% CI −0.384 to 0.600]. Lung tissues were harvested from a subset of hamsters at 4 dpi in each group. Early treatment with ETV resulted in a larger

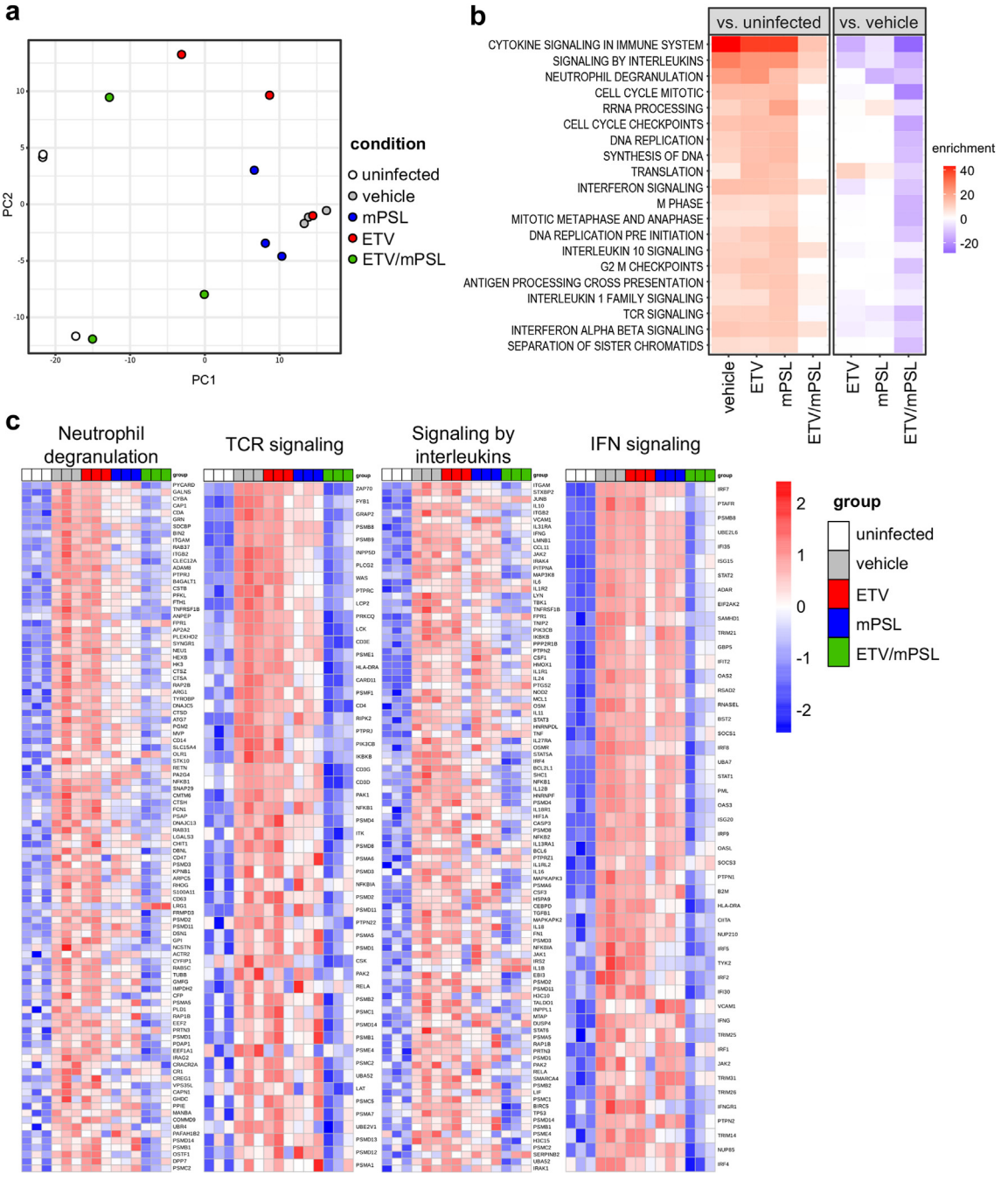

Fig. 4: **Transcriptomic signatures in the lungs of SARS-CoV-2-infected hamsters receiving therapeutic treatment.** Male hamsters were infected with 1×10^4 pfu of the SARS-CoV-2 delta variant and treated b.i.d. with ETV (200 mg/kg) and/or mPSL (10 mg/kg) at 2–3 dpi following the schedule shown in Fig. 2a. **a**, Principal component analysis of gene expression data were derived from the whole lungs of hamsters at 4 dpi. Dots indicate infected hamsters receiving vehicle (grey), mPSL (blue), ETV (red), or ETV/mPSL (green) and uninfected controls (white). The explained variance by each component was 65% for PC1 and 18% for PC2. **b**, Gene set enrichment analysis of differentially expressed genes. Upregulated (red) or downregulated (blue) gene pathways compared to uninfected control (left panel) and infected vehicle-treated hamsters (right panel) are shown. Enrichment values were calculated as $-\log_{10}$ (adjusted *P*-value), and downregulated pathways are represented with negative values. **c**, Heatmaps showing the relative expression of a panel of genes in enriched pathways. No more than 100 of the top upregulated genes in each pathway in an untreated vehicle control group compared to the uninfected control group are shown. Each column represents a single sample from the vehicle (grey), mPSL (blue), ETV (red), ETV/mPSL (green) or uninfected control group (white).

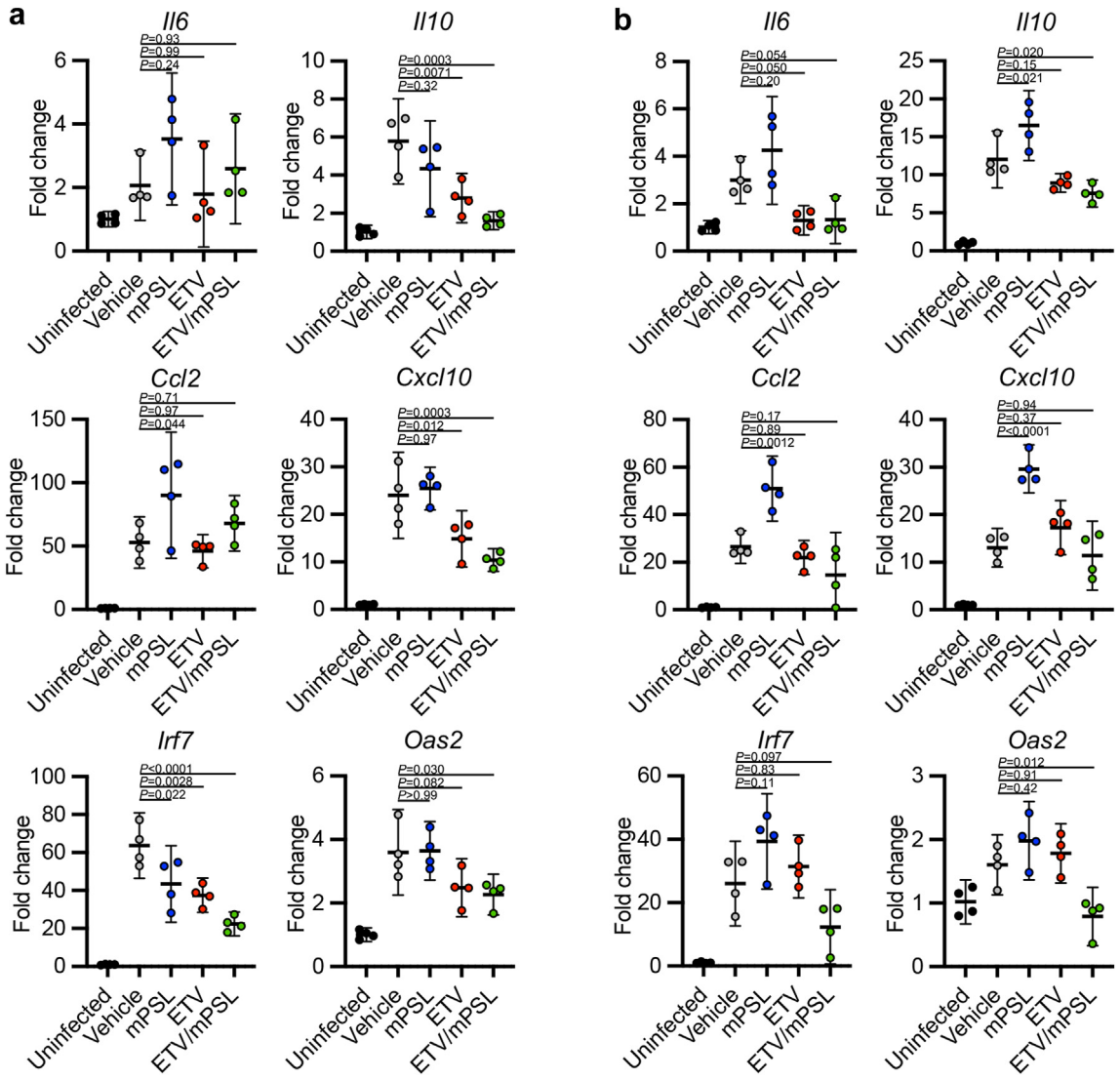

***Fig. 5*: Validation of differential gene expression associated with therapeutic treatment with ETV and mPSL. a, b**, Relative gene expression of cytokines and interferon-stimulated genes in the lungs of male hamsters at 4 (a) and 6 dpi (b). mRNA expression was quantified using a probe-based qRT-PCR assay (n = 4 for each group). Data were normalised to those of *Actb*. All graph shows mean and 95% CIs with each dot representing an individual animal. Statistics were calculated by one-way ANOVA with Tukey's test. *P* values versus vehicle-treated control are indicated in the graphs.

decrease in viral loads in the lungs (Fig. 1f and g). Although the total administration doses of ETV until 4 dpi are different between prophylactic [ETV (0 dpi)] and therapeutic [ETV (1 dpi), ETV (2 dpi)] treatment groups, the viral loads in therapeutic groups were also decreased by 1–2 orders of magnitude even when treatment was started after 2 dpi (Fig. 1f and g). On gross examination, focal congestion and haemorrhage were observed in the lungs of hamsters in the vehicle and ETV (2 dpi) groups, but such findings were limited in hamsters in the ETV (0 dpi) and ETV (1 dpi) groups (Fig. 1h). The cytokines IL-6, IL-10 and the chemokines CCL2, CXCL10 are associated with severe COVID-19, and can serve as biological markers for COVID-19 severity.[1,2] The gene expression of these cytokines and chemokines was induced in the lungs of infected hamsters at 4 dpi, and this upregulation was strongly inhibited in the ETV (0 dpi) and ETV (1 dpi) groups but only slightly inhibited in the ETV (2 dpi) group (Fig. 1i–l). These results indicate that ETV treatment reduces the viral load and ameliorates both the inflammatory state in the lungs and the clinical aspects of COVID-19, but the therapeutic effect is mitigated when ETV treatment is delayed after infection.

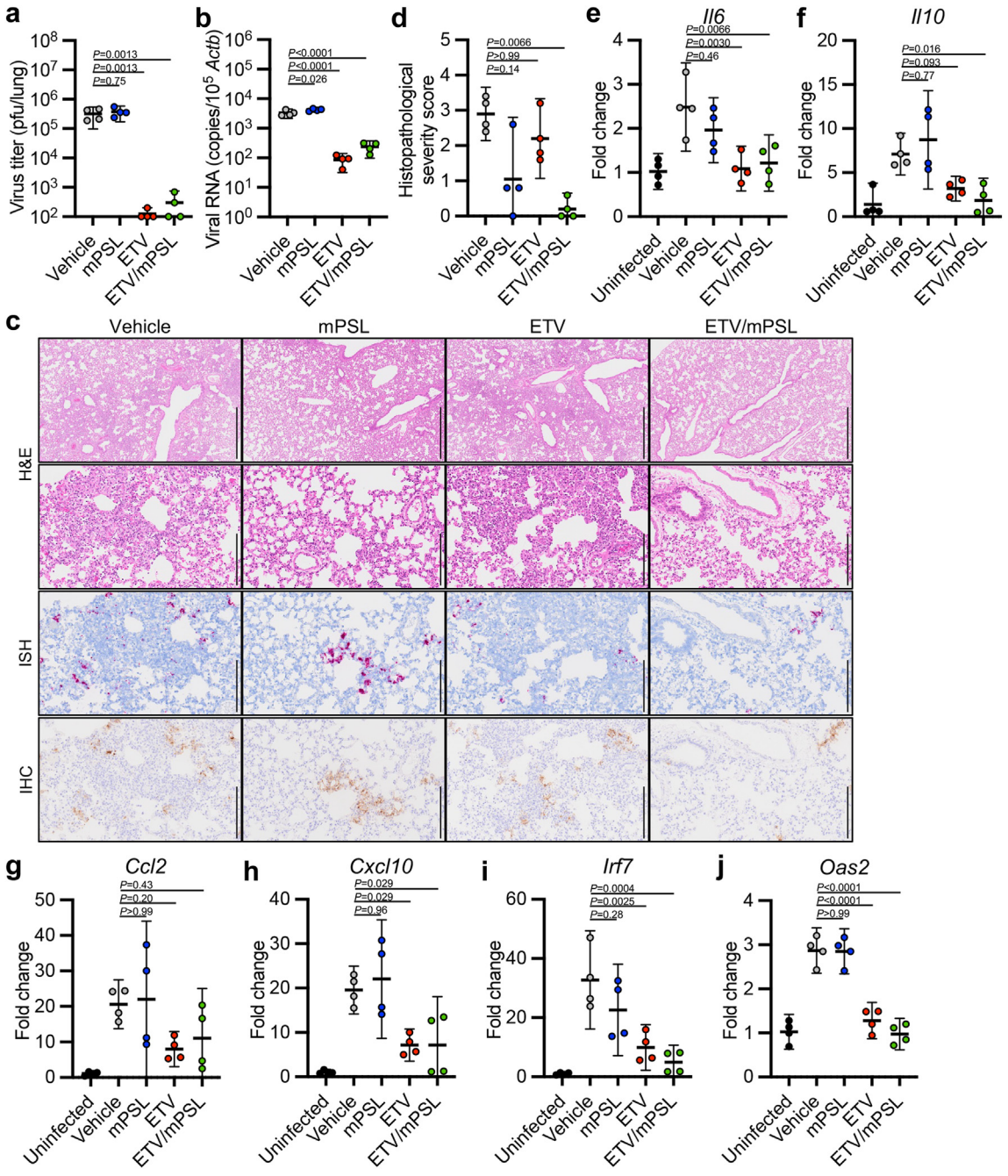

Fig. 6: **Therapeutic treatment of hamsters infected with SARS-CoV-2 omicron variant.** Male hamsters were infected with 1×10^4 pfu of the SARS-CoV-2 omicron variant XBB.1 and treated b.i.d. with ETV (200 mg/kg) and/or mPSL (10 mg/kg) at 2–3 dpi. **a**, Virus titres in hamster lungs at 4 dpi were determined by plaque assay (n = 4 for each group). **b**, Viral RNA copies in hamster lungs at 4 dpi were quantified by qRT-PCR and normalised to those of *Actb* (n = 4 for each group). **c**, Representative histopathological images of hamster lungs at 4 dpi. Upper two panels, haematoxylin and eosin staining. The third from the top panels, ISH targeting the nucleocapsid gene of SARS-CoV-2. Bottom panels, IHC targeting the nucleocapsid protein of SARS-CoV-2. Scale bars in the top panels, 1 mm. Scale bars in other panels, 200 μm. **d**, Histopathological severity score of pneumonia based on the percentage area of alveolitis in a given section (n = 4 for each group). **e–j**, Relative gene expression of *Il6* (e), *Il10* (f), *Ccl2* (g), *Cxcl10* (h), *Irf7* (i), and *Oas2* (j) in hamster lungs at 4 dpi compared to the findings in the lungs of uninfected hamsters were examined using qRT-PCR (n = 4 for each group). Data were normalised to those of *Actb*. All graph shows mean and 95% CIs with each dot representing an individual animal. Statistics were calculated by one-way ANOVA with Dunnett's test (a, b), Kruskal–Wallis test with Dunn's test (d) and one-way ANOVA with Tukey's test (e–j). *P* values versus vehicle-treated control are indicated in the graphs.

Combination therapy with ETV and mPSL accelerates the recovery from severe COVID-19

Previous studies demonstrated that the administration of anti-inflammatory corticosteroids (dexamethasone and mPSL) ameliorates pneumonia temporally but increases the viral load in hamsters infected with SARS-CoV-2.[19–21] We next examined the therapeutic effect of delayed corticosteroid treatment in hamsters infected with SARS-CoV-2. Hamsters infected with the SARS-CoV-2 delta variant were orally administered with mPSL for 2 days (2–3 dpi) and/or ETV for 5 days (2–6 dpi; Fig. 2a). Compared to vehicle-treated group, monotherapy with mPSL had little impact on body weight loss caused by infection [mean AUC difference of 11.7, 95% CI –66.0 to 89.3], but the hamsters receiving ETV/mPSL combination therapy showed the lowest body weight loss among all examined groups [mean AUC difference of –94.4, 95% CI –166 to –22.5] (Fig. 2b and c). We note that oral administration of mPSL caused slight body weight loss in uninfected hamsters (Supplementary Figure S1). Penh and Rpef at 4 dpi were improved by mPSL monotherapy [mean Penh difference of 0.892, 95% CI 0.424–1.36] and in combination with ETV [mean Penh difference of 0.970, 95% CI 0.502–1.44], whereas mPSL monotherapy aggravated the respiratory conditions in hamsters at 6 dpi [mean Penh difference of 0.0214, 95% CI –0.227 to 0.270] (Fig. 2d and e). Infectious virus and viral RNA loads in the lungs of hamsters at 4 and 6 dpi were reduced by ETV/mPSL combination therapy, but their viral loads were slightly higher than those in hamsters receiving ETV monotherapy (Fig. 2f–i). Hamsters treated with mPSL monotherapy maintained relatively high viral loads at 6 dpi compared to those in vehicle-treated hamsters, consistent with a previous study.[19] We also examined the antiviral effect of RDV monotherapy and combination therapy with mPSL in a delayed dosing protocol. Monotherapy with RDV achieved 10-fold decrease in virus titres in the lungs of hamsters, but the antiviral effect of RDV was lower than that of ETV treatments (Supplementary Figure S2). The limited antiviral effect was further reduced in the combination treatment with mPSL and has been partly explained by the high serum esterase activity, causing the metabolism of RDV.[46] Collectively, these results indicate that ETV/mPSL combination treatment exhibits high therapeutic activity and ameliorates the severity of COVID-19 without delaying virus clearance in a delayed dosing model of SARS-CoV-2 infected hamsters.

Effects of combination therapy with ETV and mPSL on lung pathology

We examined the pathological features in hamster lungs. On gross examination, focal congestion and haemorrhage were observed in the lungs of hamsters receiving monotherapy with ETV or mPSL as well as in the vehicle control at 4 dpi (Fig. 3a). In contrast, few pathological changes were observed in the lungs of animals that received ETV/mPSL combination therapy. The histopathological severity score of pneumonia was determined on the basis of inflammation, oedema, and haemorrhage as described in the Methods. Histopathological examination uncovered extensive inflammatory cell infiltration along with alveolar haemorrhage in the lungs of vehicle-treated hamsters (Fig. 3b). This severe inflammation was slightly but reduced in the lung sections of hamsters treated with mPSL or ETV monotherapy (Fig. 3c). Meanwhile, lung sections of hamsters treated with ETV/mPSL combination therapy demonstrated mild inflammation in limited legions and lower severity scores compared to the vehicle-treated animals (Fig. 3b and c). Immunohistochemical and *in situ* hybridization analyses revealed that viral antigen- and viral RNA-positive cells were distributed across extended areas of the lungs of the hamsters in the vehicle and mPSL monotherapy groups, whereas a smaller number of cells in the lungs of animals in the ETV monotherapy and ETV/mPSL combination therapy groups were positive for viral RNA/antigen (Fig. 3b). At 6 dpi, we observed severe inflammation accompanied by alveolar haemorrhage and/or pulmonary oedema in the lungs of hamsters receiving mPSL monotherapy, as well as in the vehicle control group (Fig. 3d). In contrast, the inflammation was less severe in the lungs of hamsters that received ETV monotherapy or ETV/mPSL combination therapy. The histopathological severity score for pneumonia in the mPSL monotherapy group was comparable to that of the vehicle control group (Fig. 3e). However, the score showed a slight reduction in the ETV monotherapy group and the ETV/mPSL combination therapy group. Because hamsters receiving ETV/mPSL combination therapy exhibited mild symptoms with limited inflammatory responses to the infection during the monitoring period, we evaluated seroconversion in the hamsters. Hamsters treated with vehicle, ETV monotherapy, mPSL monotherapy, and ETV/mPSL combination therapy elicited comparable neutralizing antibody titres at 18 dpi (Fig. 3f). Taken together, ETV/mPSL combination treatment restricted both viral spread and hyperinflammation in the lungs without changes in seroconversion to SARS-CoV-2, which in turn leads to a more desirable therapeutic effect compared to that of ETV or mPSL monotherapy.

Combination therapy with ETV and mPSL controls the host inflammatory response to COVID-19

SARS-CoV-2 infection induces marked and imbalanced upregulation of various cytokines, chemokines, and interferon-stimulated genes (ISGs), which are associated with COVID-19 pneumonia and disease severity. We therefore extended our analysis of the effect of treatment on gene expression profiles. The transcriptome of hamster lungs at 4 dpi was analysed by mRNA sequencing (mRNA-seq). Principal component

analysis revealed distinct gene expression signatures between uninfected and infected (vehicle-treated) hamsters (Fig. 4a). The gene expression signatures of hamsters treated with ETV/mPSL combination therapy were separated from those of hamsters treated with vehicle, ETV, or mPSL monotherapies (Fig. 4a). Consistent with the results of the histopathological examination, the differential expression of cell marker genes suggested a prominent inflammatory cell infiltration in the lungs of hamsters in the vehicle, ETV, and mPSL groups compared to that in the ETV/mPSL combination therapy group (Supplementary Figure S3). Pathway analysis of differentially expressed genes highlighted host innate immune and inflammatory responses to the infection, such as cytokine/chemokine signalling and cell cycle regulation in infected hamsters compared to uninfected hamsters (Fig. 4b, left panel). In comparison to vehicle treatment, mPSL monotherapy inhibited the upregulation of some genes enriched for neutrophil degranulation and T cell receptor (TCR) signalling, whereas ETV monotherapy had little impact on these pathways (Fig. 4b, right panel and 4c). Notably, ETV/mPSL combination therapy reverted the upregulation of genes enriched for interferon and interleukin signalling in addition to neutrophil degranulation and TCR signalling by infection (Fig. 4b and c), indicating a comprehensive effect of treatment on the host immune response to COVID-19. The magnitude of gene expression changes did show some variations among hamster individuals in same treatment groups (Fig. 4c). We validated the expression of cytokines and chemokines in hamster lungs at 4 and 6 dpi by quantitative RT-PCR (qRT-PCR; Fig. 5a and b). We also included *Oas2* and *Irf7*, which were upregulated ISGs in our transcriptome analysis and have been reported to play an essential role in inflammatory symptoms associated with COVID-19.[47,48] Consistently, the ETV/mPSL combination therapy controlled the host inflammatory response to infection. At 6 dpi, hamsters in the mPSL monotherapy group exhibited high expression of cytokines, chemokines, and ISGs (Fig. 5b), corresponding to the delay in viral clearance (Fig. 2h and i). It has been reported that IL-10 upregulates the expression of ACE2 and renders the susceptibility to SARS-CoV-2 infection to alveolar macrophages, resulting in COVID-19 progression.[49] The expression levels of IL-10 were increased from 4 to 6 dpi in hamsters and the escalation was significantly inhibited by the ETV/mPSL combination therapy (Fig. 5a and b). These results indicate that ETV/mPSL combination therapy controls both viral growth and host inflammatory responses to SARS-CoV-2 infection, leading to better outcomes for recipient animals with COVID-19.

As with human cases, male hamsters develop more severe clinical signs and lung pathology compared to females.[50] To evaluate the potential sex differences in the responses to the delayed treatments, we examined the therapeutic efficacy in female hamsters infected with the SARS-CoV-2 delta variant. Both ETV monotherapy and ETV/mPSL combination therapy decreased viral loads and inhibited the upregulation of cytokines in the lungs of female hamsters at 4 dpi (Supplementary Figure S4).

Combination therapy with ETV and mPSL for SARS-CoV-2 omicron XBB.1

Compared to the highly pathogenic SARS-CoV-2 delta variant, the currently circulating omicron variant has relatively low virulence and slow growth in the lungs, and it causes attenuated disease in hamsters.[42,45,51] As such, we investigated the effect of ETV/mPSL combination therapy against SARS-CoV-2 XBB.1, a sub-lineage of the omicron variant. Because omicron infection has little impact on body weight and respiratory parameters in hamsters,[51] we focused on the viral load and inflammation in the lungs to evaluate therapeutic efficacy. ETV monotherapy and ETV/mPSL combination therapy, but not mPSL monotherapy, reduced virus titres and viral RNA loads in the lungs of hamsters at 4 dpi (Fig. 6a and b). Histopathological examination revealed that ETV/mPSL combination therapy improved the severity score with reduced inflammatory cell infiltration and lower numbers of viral RNA/antigen-positive cells (Fig. 6c and d). In addition, mPSL monotherapy attenuated the lung pathology without decreasing the number of virus-infected cells (Fig. 6c and d). The expression of cytokines, chemokines, and ISGs in the lungs was elevated following infection, and this gene upregulation was suppressed by treatment with ETV monotherapy and in combination with mPSL, presumably due to changes in viral loads (Fig. 6e–j). These results indicate that ETV/mPSL combination therapy ameliorates pneumonia caused by the SARS-CoV-2 omicron variant, whereas ETV and mPSL monotherapies only partially improve host inflammatory responses to infection.

Discussion

Lung bronchial and alveolar epithelial cells are targets for SARS-CoV-2 infection. The infected cells release inflammatory mediators and trigger host inflammatory responses with pulmonary infiltration of immune cells, leading to COVID-19 pneumonia.[1] Therefore, inhibiting SARS-CoV-2 proliferation in the early phase of infection prevents hyperinflammation and mitigates the severity of the disease. In this study, hamsters receiving delayed treatment with ETV from 2 dpi showed greater weight loss, more severe respiratory conditions, and higher expression of cytokines and chemokines than hamsters receiving ETV in an earlier phase of infection, indicating that delayed antiviral treatment resulted in reduced therapeutic efficacy. It is suggested that controlling the host inflammatory response is an essential factor for a better performance of delayed therapy for COVID-19.

Because viral loads have been reported to peak around 2 dpi in the lungs of hamsters experimentally inoculated with SARS-CoV-2,[52,53] drug administration was initiated in our delayed protocol after substantial viral proliferation, which is associated with the stimulation of host inflammatory responses and lung pathology.

Previous studies demonstrated the lower replication competence and pathogenicity of omicron variants in the lungs.[42,45,51] In contrast to the infection with the delta variant, ETV monotherapy inhibited the upregulations of the pro-inflammatory cytokine IL-6, whereas it had limited impact on the histopathological severity of pneumonia in the lungs of hamsters at 4 dpi with the omicron variant XBB.1, suggesting that the attenuated infection may be more susceptible to antiviral monotherapy. We can conclude that lower viral road and IL-6 levels following ETV monotherapy will contribute to the efficient viral clearance, improved lung conditions and overall better outcomes in COVID-19.

Our mRNA-seq analysis revealed that mPSL monotherapy suppressed neutrophil and T cell activation, suggesting that these phenotypes contribute to the amelioration of COVID-19-induced lung pathology. Consistent with our findings, it has been reported that dexamethasone induced the immunosuppression of neutrophils in patients with COVID-19.[54] Conversely, mPSL monotherapy was associated with an increased viral load, delayed viral clearance, and prolonged upregulations of several types of cytokines and chemokines in the lungs. These paradoxical effects of steroidal anti-inflammatory drugs were also recognised in a previous study using SARS-CoV-2-infected hamsters.[19] Furthermore, treatment with steroidal anti-inflammatory drugs had varied and inconsistent effects on the expression of cytokine and chemokine genes in various studies, presumably because of differences in the time course, administration route, and doses of the anti-inflammatory drugs.[19–21] Our histopathological examination revealed that mPSL monotherapy partially improved the lung pathology in hamsters infected with the omicron variant, but not in those infected with the highly pathogenic delta variant. These results highlight the complexity and difficulty of treatment with steroidal anti-inflammatory drugs for COVID-19.

Theoretically, the antiviral effects of drugs could compensate for the undesirable delay in viral clearance induced by treatment with anti-inflammatory drugs in COVID-19. Compared to the effects of ETV or mPSL monotherapies, the combination therapy controlled a wide range of host inflammatory responses, improved the lung pathology, and ameliorated clinical aspects of COVID-19 in hamsters. Furthermore, the combination treatment was effective in infection with both highly pathogenic delta and circulating omicron variants. We propose a model in which ETV/mPSL combination treatment suppressed pulmonary inflammation without a delay in virus clearance and achieved strong therapeutic efficacy following delayed treatment in SARS-CoV-2-infected hamsters (Supplementary Figure S5). In conclusion, our study demonstrates that combination therapy with antiviral and anti-inflammatory drugs could provide a potent therapeutic option for treatment of COVID-19.

However, we noted some limitations and confounding factors in this study. First, we examined the performance of combination therapy using a single set of oral antiviral/anti-inflammatory drugs. Nirmatrelvir and molnupiravir have been widely used as oral antiviral drugs for COVID-19, and they are candidates for further investigation of antiviral/anti-inflammatory combination therapy. Second, we did not consider the effect of drug–drug interactions between ETV and mPSL in hamsters receiving this combination therapy as a confounding factor that may influence the therapeutic effect. A clinical study reported that ETV increases the area under the plasma concentration-time curve of dexamethasone, but ETV has no clinically meaningful effect on the pharmacokinetics of prednisolone in humans.[55] We therefore did not include dexamethasone in the combination regimen in this study. Third, this study was conducted using hamsters experimentally inoculated with SARS-CoV-2. Although hamsters mimic many aspects of human COVID-19, species specific immune response to the infection and treatment may be a potential confounding factor. We also could not exclude the experimental settings including the virus strain, virus titre, and inoculum size alter the course and severity of COVID-19.[56] Most of our studies were conducted using the highly pathogenic delta variant with a large inoculum volume, leading to acute and severe infection. This severe COVID-19 model has an advantage of low individual variation, but it could be less sensitive to observe other therapeutic treatments.

In summary, our study has revealed the advantage of combination therapy with ETV and mPSL from the perspective of lung pathology and host inflammatory responses. Since patients can easily receive oral medications, combination therapy with oral antiviral and anti-inflammatory drugs could serve as a practical and potent treatment option for COVID-19.

Contributors

M.S. and T.Sugi designed the study. M.S., S.I., Y.H., S.K., K.K., Y.I., K.T., M.K., H.K., T.A., K.I., S.T., Y.O. and H.S. performed the experiments. M.S., T.Sugi, S.I., Y.H. and T.Suzuki analysed the data. M.S., A.S., J.Y., Y.O. and H.S. supervised this study. H.N. and K.M. contributed to critical resources and methodology. M.S., T.Sugi, S.K., W.W.H. and H.S. wrote the original draft. M.S., T.Suzuki and H.S. verified the underlying data. All authors read and approved the final version of the manuscript.

Data sharing statement

Raw mRNA-seq data were deposited to DDBJ with accession IDs DRR477693-DRR477707. All data of this study are available from the corresponding author upon request.

Declaration of interests

SK, HN and ST owns stocks in Shionogi & Co., Ltd. KM, YO and HS are involved in joint research contract between Shionogi & Co., Ltd., and Hokkaido University. MS has received fees for speaker bureaus from Shionogi & Co., Ltd. MS, HN, ST and HS are inventors on patent application numbers PCT/JP2022/035803 (MS, HN, ST and HS), PCT/JP2022/6495 and PCT/JP2022/6496 (MS) submitted by Shionogi & Co., Ltd., and Hokkaido University that covers ETV. SI has received grants from Japan Society for the Promotion of Science. TS has received grants from Japan Society for the Promotion of Science and Japan Agency for Medical Research and Development. HS has received grants from Japan Agency for Medical Research and Development. The remaining authors have no potential competing interests to declare.

Acknowledgements

We thank the National Institute of Infectious Diseases, Japan for providing the SARS-CoV-2 variants and Dr. Kei Sato in Tokyo University, Japan for supporting pulmonary function tests using a plethysmography system. We also thank Yuko Sato and Seiya Ozono for technical assistance. The authors SK, KK, HN, ST and AS are employees of Shionogi & Co., Ltd. This work was supported by the Japan Agency for Medical Research and Development (AMED) under Grant numbers JP23wm0125008, JP223fa627005 and JP23fk0108637; Japan Science and Technology Agency (JST) Moonshot R&D under Grant number JPMJMS2025; the World-leading Innovative and Smart Education (WISE) Program from the Ministry of Education, Culture, Sports, Science and Technology (MEXT), Japan under Grant number 1801; and the Promotion Project for Young Investigators in Hokkaido University. YO and HS have received research funding support from Shionogi & Co. Ltd.

Appendix A. Supplementary data

Supplementary data related to this article can be found at https://doi.org/10.1016/j.ebiom.2023.104950.

References

1 Lamers MM, Haagmans BL. SARS-CoV-2 pathogenesis. *Nat Rev Microbiol*. 2022;20:270–284.
2 Hsu RJ, Yu WC, Peng GR, et al. The role of cytokines and chemokines in severe acute respiratory syndrome coronavirus 2 infections. *Front Immunol*. 2022;13:832394.
3 Merad M, Blish CA, Sallusto F, Iwasaki A. The immunology and immunopathology of COVID-19. *Science*. 2022;375:1122–1127.
4 Diamond MS, Kanneganti TD. Innate immunity: the first line of defense against SARS-CoV-2. *Nat Immunol*. 2022;23:165–176.
5 COVID-19 treatment guidelines panel. Coronavirus disease 2019 (COVID-19) treatment guidelines. National Institutes of Health. Available at: https://www.covid19treatmentguidelines.nih.gov/. Accessed May 22, 2023.
6 Jayk Bernal A, Gomes da Silva MM, Musungaie DB, et al. Molnupiravir for oral treatment of Covid-19 in nonhospitalized patients. *N Engl J Med*. 2022;386:509–520.
7 Hammond J, Leister-Tebbe H, Gardner A, et al. Oral nirmatrelvir for high-risk, nonhospitalized adults with Covid-19. *N Engl J Med*. 2022;386:1397–1408.
8 Mukae H, Yotsuyanagi H, Ohmagari N, et al. Efficacy and safety of ensitrelvir in patients with mild-to-moderate coronavirus disease 2019: the phase 2b part of a randomized, placebo-controlled, phase 2/3 study. *Clin Infect Dis*. 2023;76:1403–1411.
9 Horby P, Lim WS, Emberson JR, et al. Dexamethasone in hospitalized patients with Covid-19. *N Engl J Med*. 2021;384:693–704.
10 Hong S, Wang H, Li S, Liu J, Qiao L. A systematic review and meta-analysis of glucocorticoids treatment in severe COVID-19: methylprednisolone versus dexamethasone. *BMC Infect Dis*. 2023;23:290.
11 Covello RD, Pasin L, Fresilli S, et al. Meta-analysis of glucocorticoids for Covid-19 patients not receiving oxygen. *NEJM Evid*. 2023;2:EVIDoa2200283.
12 Crothers K, DeFaccio R, Tate J, et al. Dexamethasone in hospitalised COVID-19 patients not on intensive respiratory support. *Eur Respir J*. 2022;60:2102532.
13 Marrone A, Nevola R, Sellitto A, et al. Remdesivir plus dexamethasone versus dexamethasone alone for the treatment of coronavirus disease 2019 (COVID-19) patients requiring supplemental O2 therapy: a prospective controlled nonrandomized study. *Clin Infect Dis*. 2022;75:e403–e409.
14 Kalil AC, Patterson TF, Mehta AK, et al. Baricitinib plus remdesivir for hospitalized adults with Covid-19. *N Engl J Med*. 2021;384:795–807.
15 Uraki R, Kiso M, Imai M, et al. Therapeutic efficacy of monoclonal antibodies and antivirals against SARS-CoV-2 Omicron BA.1 in Syrian hamsters. *Nat Microbiol*. 2022;7:1252–1258.
16 Rosenke K, Hansen F, Schwarz B, et al. Orally delivered MK-4482 inhibits SARS-CoV-2 replication in the Syrian hamster model. *Nat Commun*. 2021;12:2295.
17 Abdelnabi R, Foo CS, Jochmans D, et al. The oral protease inhibitor (PF-07321332) protects Syrian hamsters against infection with SARS-CoV-2 variants of concern. *Nat Commun*. 2022;13:719.
18 Sasaki M, Tabata K, Kishimoto M, et al. S-217622, a SARS-CoV-2 main protease inhibitor, decreases viral load and ameliorates COVID-19 severity in hamsters. *Sci Transl Med*. 2023;15:eabq4064.
19 Ye ZW, Yuan S, Chan JF, et al. Beneficial effect of combinational methylprednisolone and remdesivir in hamster model of SARS-CoV-2 infection. *Emerg Microbes Infect*. 2021;10:291–304.
20 Yuan L, Zhou M, Ma J, et al. Dexamethasone ameliorates severe pneumonia but slightly enhances viral replication in the lungs of SARS-CoV-2-infected Syrian hamsters. *Cell Mol Immunol*. 2022;19:290–292.
21 Wyler E, Adler JM, Eschke K, et al. Key benefits of dexamethasone and antibody treatment in COVID-19 hamster models revealed by single-cell transcriptomics. *Mol Ther*. 2022;30:1952–1965.
22 Sasaki M, Uemura K, Sato A, et al. SARS-CoV-2 variants with mutations at the S1/S2 cleavage site are generated in vitro during propagation in TMPRSS2-deficient cells. *PLoS Pathog*. 2021;17:e1009233.
23 Uemura K, Sasaki M, Sanaki T, et al. MRC5 cells engineered to express ACE2 serve as a model system for the discovery of antivirals targeting SARS-CoV-2. *Sci Rep*. 2021;11:5376.
24 Unoh Y, Uehara S, Nakahara K, et al. Discovery of S-217622, a noncovalent oral SARS-CoV-2 3CL protease inhibitor clinical candidate for treating COVID-19. *J Med Chem*. 2022;65:6499–6512.
25 Pharmaceutical Evaluation Division PSaEHB, Japan. *Report on the deliberation results. Xocova tablets 125 mg*; 2022. Available at: https://www.pmda.go.jp/files/000249828.pdf. Accessed October 6, 2023.
26 Zivcec M, Safronetz D, Haddock E, Feldmann H, Ebihara H. Validation of assays to monitor immune responses in the Syrian golden hamster (Mesocricetus auratus). *J Immunol Methods*. 2011;368:24–35.
27 Bricker TL, Darling TL, Hassan AO, et al. A single intranasal or intramuscular immunization with chimpanzee adenovirus-vectored SARS-CoV-2 vaccine protects against pneumonia in hamsters. *Cell Rep*. 2021;36:109400.
28 Shirato K, Nao N, Katano H, et al. Development of genetic diagnostic methods for detection for novel coronavirus 2019 (nCoV-2019) in Japan. *Jpn J Infect Dis*. 2020;73:304–307.
29 Ewels PA, Peltzer A, Fillinger S, et al. The nf-core framework for community-curated bioinformatics pipelines. *Nat Biotechnol*. 2020;38:276–278.
30 Dobin A, Davis CA, Schlesinger F, et al. STAR: ultrafast universal RNA-seq aligner. *Bioinformatics*. 2013;29:15–21.
31 Cunningham F, Allen JE, Allen J, et al. Ensembl 2022. *Nucleic Acids Res*. 2022;50:D988–D995.
32 Patro R, Duggal G, Love MI, Irizarry RA, Kingsford C. Salmon provides fast and bias-aware quantification of transcript expression. *Nat Methods*. 2017;14:417–419.
33 Soneson C, Love MI, Robinson MD. Differential analyses for RNA-seq: transcript-level estimates improve gene-level inferences. *F1000Res*. 2015;4:1521.
34 Love MI, Huber W, Anders S. Moderated estimation of fold change and dispersion for RNA-seq data with DESeq2. *Genome Biol*. 2014;15:550.
35 Van den Berge K, Perraudeau F, Soneson C, et al. Observation weights unlock bulk RNA-seq tools for zero inflation and single-cell applications. *Genome Biol*. 2018;19:24.
36 Mootha VK, Lindgren CM, Eriksson KF, et al. PGC-1alpha-responsive genes involved in oxidative phosphorylation are coordinately downregulated in human diabetes. *Nat Genet*. 2003;34:267–273.

37 Wu T, Hu E, Xu S, et al. clusterProfiler 4.0: a universal enrichment tool for interpreting omics data. *Innovation*. 2021;2:100141.
38 Raudvere U, Kolberg L, Kuzmin I, et al. Profiler: a web server for functional enrichment analysis and conversions of gene lists (2019 update). *Nucleic Acids Res*. 2019;47:W191–W198.
39 Gillespie M, Jassal B, Stephan R, et al. The reactome pathway knowledgebase 2022. *Nucleic Acids Res*. 2022;50:D687–D692.
40 Zhang X, Lan Y, Xu J, et al. CellMarker: a manually curated resource of cell markers in human and mouse. *Nucleic Acids Res*. 2019;47:D721–D728.
41 Yamasoba D, Kimura I, Nasser H, et al. Virological characteristics of the SARS-CoV-2 Omicron BA.2 spike. *Cell*. 2022;185:2103–2115.e19.
42 Halfmann PJ, Iida S, Iwatsuki-Horimoto K, et al. SARS-CoV-2 Omicron virus causes attenuated disease in mice and hamsters. *Nature*. 2022;603:687–692.
43 Uraki R, Halfmann PJ, Iida S, et al. Characterization of SARS-CoV-2 Omicron BA.4 and BA.5 isolates in rodents. *Nature*. 2022;612:540–545.
44 Saito A, Irie T, Suzuki R, et al. Enhanced fusogenicity and pathogenicity of SARS-CoV-2 Delta P681R mutation. *Nature*. 2022;602:300–306.
45 Yuan S, Ye ZW, Liang R, et al. Pathogenicity, transmissibility, and fitness of SARS-CoV-2 Omicron in Syrian hamsters. *Science*. 2022;377:428–433.
46 Sheahan TP, Sims AC, Graham RL, et al. Broad-spectrum antiviral GS-5734 inhibits both epidemic and zoonotic coronaviruses. *Sci Transl Med*. 2017;9:eaal3653.
47 Lee D, Le Pen J, Yatim A, et al. Inborn errors of OAS-RNase L in SARS-CoV-2-related multisystem inflammatory syndrome in children. *Science*. 2023;379:eabo3627.
48 Zhang Q, Bastard P, Liu Z, et al. Inborn errors of type I IFN immunity in patients with life-threatening COVID-19. *Science*. 2020;370:eabd4570.
49 Mitsui Y, Suzuki T, Kuniyoshi K, et al. Expression of the read-through transcript CiDRE in alveolar macrophages boosts SARS-CoV-2 susceptibility and promotes COVID-19 severity. *Immunity*. 2023;56:1939–1954.e12.
50 Dhakal S, Ruiz-Bedoya CA, Zhou R, et al. Sex differences in lung imaging and SARS-CoV-2 antibody responses in a COVID-19 golden Syrian hamster model. *mBio*. 2021;12:e0097421.
51 Tamura T, Ito J, Uriu K, et al. Virological characteristics of the SARS-CoV-2 XBB variant derived from recombination of two Omicron subvariants. *Nat Commun*. 2023;14:2800.
52 Campos RK, Camargos VN, Azar SR, Haines CA, Eyzaguirre EJ, Rossi SL. SARS-CoV-2 infects hamster testes. *Microorganisms*. 2021;9:1318.
53 Sia SF, Yan LM, Chin AWH, et al. Pathogenesis and transmission of SARS-CoV-2 in golden hamsters. *Nature*. 2020;583:834–838.
54 Sinha S, Rosin NL, Arora R, et al. Dexamethasone modulates immature neutrophils and interferon programming in severe COVID-19. *Nat Med*. 2022;28:201–211.
55 Shimizu R, Sonoyama T, Fukuhara T, et al. Evaluation of the drug-drug interaction potential of ensitrelvir fumaric acid with cytochrome P450 3A substrates in healthy Japanese adults. *Clin Drug Investig*. 2023;43:335–346.
56 Handley A, Ryan KA, Davies ER, et al. SARS-CoV-2 disease severity in the golden Syrian hamster model of infection is related to the volume of intranasal inoculum. *Viruses*. 2023;15:748.